remote sensing

MDPI

Article

Impacts of Spatial and Temporal Resolution on Remotely Sensed Corn and Soybean Emergence Detection

Feng Gao [1,*], Martha Anderson [1] and Rasmus Houborg [2]

[1] Hydrology and Remote Sensing Laboratory, U.S. Department of Agriculture, Agricultural Research Service, 10300 Baltimore Avenue, Beltsville, MD 20705, USA; martha.anderson@usda.gov
[2] Planet Labs Public Benefit Corporation, San Francisco, CA 94107, USA; rasmus.houborg@planet.com
* Correspondence: feng.gao@usda.gov

Abstract: Crop emergence is critical for crop growth modeling, crop condition monitoring, and crop yield estimation. Ground collections of crop emergence dates are time-consuming and can only include limited fields. Remote sensing time series have been used to detect crop emergence. However, the impacts of the temporal and spatial resolutions of these time series on crop emergence detection have not been thoroughly evaluated. This paper assesses corn and soybean emergence detection using various remote sensing datasets (i.e., VENμS, Planet Fusion, Sentinel-2, Landsat, and Harmonized Landsat and Sentinel-2 (HLS)) with diverse spatial and temporal resolutions. The green-up dates from the remote sensing time series are detected using the within-season emergence (WISE) algorithm and assessed using ground emergence observations and planting records of corn, soybeans, and alfalfa from the Beltsville Agricultural Research Center (BARC) fields in Maryland, USA, from 2019 to 2023. Our results showed that most emergence events (~95%) could be detected when the frequency of usable observations reached ten days or less. Planet Fusion captured all crop emergences and outperformed other datasets, with a mean difference (MD) of <1 day, a mean absolute difference (MAD) of <5 days, and a root mean square error (RMSE) of <6 days compared to the ground-observed emergence dates. The HLS and Sentinel-2 time series captured most emergences of corn and soybeans with MD < 3 days, MAD < 7 days, and RMSE < 9 days. Landsat detected less than half of the crop emergences in recent years when both Landsat-8 and -9 were available. In our study area, temporal revisit plays a more crucial role in emergence detection than spatial resolution. Spatial resolutions from 5 to 30 m are suitable for field-level summaries in the study area. However, the 30 m HLS lacked sub-field details in fields with mixed cropping systems. The findings from this study could benefit remotely sensed crop emergence detection from local to regional scales.

Keywords: crop phenology; crop condition; Harmonized Landsat and Sentinel-2; Planet Fusion; time series analysis; within-season detection

check for updates

Citation: Gao, F.; Anderson, M.; Houborg, R. Impacts of Spatial and Temporal Resolution on Remotely Sensed Corn and Soybean Emergence Detection. *Remote Sens.* **2024**, *16*, 4145. https://doi.org/10.3390/rs16224145

Academic Editors: Francesco Pirotti and Mitsunori Yoshimura

Received: 18 September 2024
Revised: 1 November 2024
Accepted: 4 November 2024
Published: 7 November 2024

Copyright: © 2024 by the authors. Licensee MDPI, Basel, Switzerland. This article is an open access article distributed under the terms and conditions of the Creative Commons Attribution (CC BY) license (https://creativecommons.org/licenses/by/4.0/).

1. Introduction

Crop emergence (VE stage) marks the initial phase of crop vegetative growth. Accurate determination of crop emergence dates is critical for crop growth modeling, crop condition monitoring, and crop yield estimation [1,2]. Crop growth models require precise planting or sowing dates to simulate crop growth, but these dates are often difficult to obtain over a large area. However, planting dates are intrinsically linked to crop emergence and weather conditions [3–5]. Crop emergence dates can be backcasted to planting dates or incorporated directly into crop growth models. Moreover, information on crop emergence can improve crop condition monitoring by aligning crop emergence dates from different years [6]. Furthermore, crop emergence dates determine the crop growth period and could be related to crop yields [7]. Consequently, understanding crop emergence is essential for research and practical agricultural applications.

Crop emergence dates at the field scale depend on temperature, soil conditions, and farmers' decisions (e.g., machine and labor availability) on planting dates [8]. Crop emergence dates vary yearly and geographically. For example, the US Corn Belt experienced a historically wet spring in 2019, and summer crops were planted 1–4 weeks later than usual [9]. These variations highlight the sensitivity of crop emergence to environmental factors and farmer planting decisions. It can be challenging to collect crop planting and emergence dates over a large area for individual fields.

Conventionally, crop emergence dates can be visually observed on the ground. The United States Department of Agriculture (USDA) National Agricultural Statistics Service (NASS) provides weekly crop progress reports on crop emergence through ground-based surveys at the state level and the 9 km gridded layer [9]. These surveys gather information from farmers and agricultural professionals to track the progress of crops throughout the growing season, including the emergence stage. However, ground data collection is time-consuming, requiring personnel to visit numerous fields to gather information. The emergence stage occurs quickly, making it difficult to observe and record emergence events in near-real time across a wide area. The state-level reports on crop growth stages from NASS lack information about spatial variability within the state. The 9 km gridded layer is too coarse for crop modeling or application at the field scale.

In addition to traditional ground-based methods, high-resolution phenocams offer more detailed insights into crop phenology [10]. The USDA Long-Term Agroecosystem Research (LTAR) Phenocam network includes 80 cameras to monitor cropland and pastures [11]. These cameras capture images at frequent intervals, allowing for the precise monitoring of crop development [12]. However, while phenocams provide valuable data, their coverage is still limited to specific locations over cropland.

Satellite remote sensing data have been used to identify crop emergence by detecting crop green-up dates based on vegetation index (VI) time series. Various remote sensing algorithms utilize different methodologies for land surface phenology detection [13]. For instance, the Collection 6 Moderate-Resolution Imaging Spectroradiometer (MODIS) Land Cover Dynamic product defines the green-up date as the point when vegetation reaches 15% of its maximum greenness amplitude [14], while the Collection 5 MODIS and VIIRS land surface phenology use the curvature-based approach [15–17]. The Harmonized Landsat and Sentinel-2 (HLS) phenology products adopted and refined the Collection 6 MODIS phenology algorithm [18]. Deines et al. [4] used a machine learning approach and retrospectively generated annual planting date maps over the United States Corn Belt using Landsat from 2000 to 2020. Since high-resolution data are usually temporally sparse, Gao et al. [19] used a data fusion approach to analyze crop phenology and detected green-up dates at the V2–V3 stage. These phenology algorithms often require multiple years of time series data to produce the target (middle) year green-up dates. These retrospective approaches are also referred to as after-season methods because green-up dates are generated 6 to 12 months after the end of the growing season. This is too late for in-season applications.

In recent research, we developed a within-season emergence (WISE) algorithm capable of detecting crop emergence within 1–3 weeks after it occurs [20,21]. Unlike traditional phenology algorithms, WISE is a near-real-time algorithm that uses recently available observations and does not require a complete year of vegetation index time series. The WISE algorithm has been partially validated using ground-observed crop emergences and phenocam photos. The validation results show that the green-up dates detected using the WISE algorithm are closely aligned with the emergence dates. For instance, the green-up dates detected using Vegetation and Environment Monitoring on a New Micro-Satellite (VENμS) data closely matched the post-emergence dates in corn and soybean crops (between the VE and V1 stages) observed over experimental agricultural fields in Maryland, USA, in 2019 [20]. In another study, the green-up dates derived from HLS datasets were found to be close to the VE stage days, with a bias of 3 days and a mean absolute difference of 7 days, using LTAR phenocams and NASS state-level crop progress reports [21]. A comprehensive review paper summarized the progress of land surface

phenology algorithms and data products using remote sensing time series [22]. Notably, the green-up dates defined by remote sensing algorithms are different from the physiological crop emergence dates [22]. In this paper, we utilize green-up dates for remote sensing detection and emergence dates for ground observations, acknowledging the discrepancies between remote sensing-derived green-up dates and traditional ground-based observations of crop emergence.

Since the WISE algorithm has been partially validated and assessed using various remote sensing data sources [20,21], we use it in this paper to evaluate the impact of crop emergence detection from varied remote sensing perspectives with new ground VE observations from 2022 and 2023 and planting records from 2019 to 2023. Here, we build on prior studies with WISE by comparing its performance across six remote datasets (VENμS, Planet Fusion, Sentinel-2 10-m, HLS S30, HLS L30, and HLS) with varying spatial and temporal characteristics. We examine VENμS, Sentinel-2, and HLS, used in prior studies (2019 only), and include new analyses with the Planet data from 2019 to 2023.

Despite the effectiveness of VENμS and HLS data in near-real-time detection of crop emergence, detecting crop emergence using remote sensing remains challenging during early spring, when signals related to crop emergence are subtle and affected by factors like soil moisture and crop residues. Additionally, cloud and snow cover during the early growing season can obscure observations, leading to potential gaps around crop emergence dates. Operational implementation requires a better understanding of various influencing factors, including temporal and spatial resolutions and field-level aggregation methods, to ensure reliable and accurate monitoring of crop emergence using remote sensing techniques. However, these impacts on VE detection have not been fully understood due to the lack of continuous observations.

The main objective of this study is to assess the impact of spatial and temporal resolutions in crop emergence detection from the various remote sensing time series, especially the daily Planet Fusion data, using ground observations and planting records. A secondary objective is to assess the capability of emergence detection regarding corn and soybeans, as well as a special alfalfa case, with multiple green-ups during the growing season, using several common remote sensing datasets. Section 2 describes the WISE algorithm and the datasets used, which come with varying spatial and temporal resolutions. Section 3 compares green-up dates from these datasets to ground emergence observations and farm planting records obtained from experimental agricultural fields in Maryland, USA. Specifically, Sections 3.1–3.3 assess the impact of temporal resolution, and Section 3.4 evaluates the impact of spatial resolution. Section 4 discusses the pros and cons of different datasets, especially the commercial Planet Fusion data (daily, 3 m) and the freely available HLS data (2–4 days, 30 m), given their widespread availability and potential utility in agricultural monitoring applications.

2. Materials and Methods

2.1. Study Area and Field Observations

The Beltsville Agricultural Research Center (BARC) is a USDA agricultural research site in Maryland, USA, spanning approximately 2670 hectares (ha) of diverse landscapes, including agricultural fields, pastures, woodlands, and wetlands. Within the expansive grounds of BARC, a wide array of crop types is cultivated, encompassing both winter and summer crops. The area includes fields ranging from small plots to extensive areas exceeding 20 hectares. The fields are diverse regarding planting and emergence dates, rendering the BARC an ideal location for the assessment of crop emergence dynamics. The site's complicated agricultural environment provides researchers with valuable opportunities to study and analyze the factors influencing crop emergence across different crop types and field sizes.

Crop emergence dates were thoroughly observed in selected corn and soybean fields within BARC, totaling 47 field-year observations. Frequent field visits were conducted around the emergence time. The crop emergence stage covers the period from the ap-

pearance of the first leaf above the soil surface until the start of the V1 stage. We used the first date of the VE stage as the ground-observed crop emergence date in validation. These observations spanned across multiple years, including 16 fields in 2019, 19 in 2022, and 12 in 2023. The fields varied from 2.5 to 16.5 hectares, with a median field size of 7.0 hectares. An alfalfa field with four harvests and green-ups during the growing season was also observed in 2019. Alfalfa is a challenging case for both remote sensing algorithms and datasets. The extensive ground observations provide a comprehensive basis for the analysis of emergence dates across different years and fields.

In addition, 115 planting dates for corn and soybean were extracted from the BARC farm operation database from 2019 to 2023. This date information covers 42 fields used for BARC yield mapping, as documented by Dulaney et al. [23]. The field sizes associated with these planting records were slightly larger than those of the crop emergence observation fields, ranging from 3.3 to 17.3 hectares, with a median field size of 7.4 hectares.

Figure 1 illustrates the geographical location of the study area in Eastern Maryland, USA, highlighting the fields with ground observations of crop emergence and planting records. The study area encompasses approximately 11.8 km by 6.8 km and represents a typical area in the mid-Atlantic region. This spatial extent and the varying field sizes provide a representative sample for the assessment of crop emergence dynamics and planting practices in the broader agricultural context of the area.

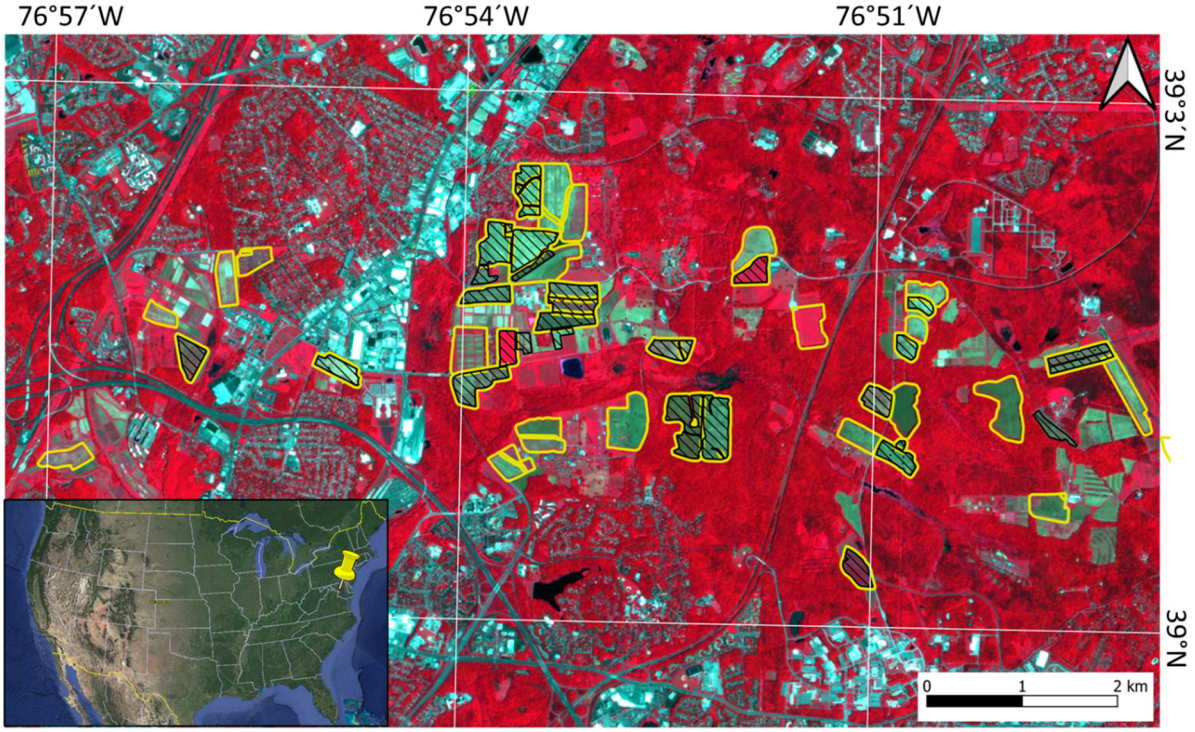

Figure 1. The BARC study area and fields are shown on the Planet Fusion composite image for 15 June 2022 (inset US figure from Google Earth). Fields with recorded planting dates are shown in yellow polygons. The fields with crop emergence observations in 2019, 2022, and 2023 are highlighted with hashed black lines.

Table 1 summarizes the fields with observed emergence dates and recorded planting dates for corn and soybeans. A total of 33 records (field-years) had both planting dates and observed crop emergence dates in 2019, 2022, and 2023. The emergence dates in these years varied from day 123 (May 3) to 199 (July 18), while the planting dates ranged from day 115 (April 25) to 194 (July 13). The days between planting and emergence varied from 2 to 13 days, with a median value of 8 days. Both the observed emergence and planting dates

over the experimental fields spanned over 2.5 months, providing an extensive range, ideal for testing algorithms and evaluating remote sensing datasets.

Table 1. The observed crop emergence and recorded planting fields and the range of dates.

Crop Type	Year	Number of Emergence Observations	Range of Emergence Dates (DOY)	Number of Planting Records	Range of Planting Dates (DOY)
Corn	2019	8	123–172	14	115–170
	2020	NA	NA	12	135–143
	2021	NA	NA	15	117–127
	2022	9	133–159	11	123–152
	2023	6	139–158	10	131–152
Soybean	2019	8	150–188	15	137–192
	2020	NA	NA	12	143–188
	2021	NA	NA	7	133–194
	2022	10	138–199	9	131–187
	2023	6	139–167	10	130–159

Daily minimum and maximum temperatures for BARC were obtained from DayMet [24] and then used to compute growing degree days (GDD) for the evaluation of green-up dates after planting.

2.2. Remote Sensing Data Sources

We evaluated six remote sensing datasets with varying spatial and temporal resolutions. Table 2 summarizes these datasets, including VENμS, Planet Fusion, Landsat, Sentinel-2 (at 10 and 30 m resolutions), and HLS. The table lists the temporal revisit days and the frequency of usable observations. The temporal revisit represents the frequency of satellite revisits in days. The frequency of usable observations in the table shows the actual temporal frequency of usable (i.e., cloud-free and snow-free) observations from 2019 to 2023. The frequency of usable observations could be much lower than the number of satellite revisits and is a more useful metric for analyzing the detection rate of crop emergence.

Table 2. Six remote sensing datasets used in this study (frequencies of usable observations are field-level averages, except for Planet data, which were averaged before generating daily observations, and for the 10 m Sentinel-2, whose statistics are based on entire images).

Data Source	Planet Fusion	VENμS	Sentinel-2	HLS-L30	HLS-S30	HLS (L&S)
Spatial Resolution	3 m	5 m	10 m		30 m	
Revisit (days)	1	2	5	8–16	5	3–4
Frequency of Usable Observations (in days)						
2019	3.5	7.4	10.5	42.4	10.3	8.3
2020	4.1	unavail	unused	55.3	9.8	8.3
2021	2.3	unavail	unused	28.7	8.1	6.3
2022	2.8	unavail	unused	18.3	9.2	6.1
2023	3.3	unavail	unused	19.5	10.0	6.6

VENμS is a joint project of the Israeli Space Agency and the French National Centre for Space Studies, which acquires imagery over 123 selected sites across the globe [25]. The BARC is one of the selected VENμS study sites, with a full year of image collection in 2019.

The VENμS time series images were used in developing the original WISE algorithm [20]. VENμS is a high-quality dataset with multispectral bands. Although the theoretical revisit is two days, the temporal frequency of usable observations was 7.4 days, not much denser than HLS (8.3 days). We used the 5 m surface reflectance data in this study. The original WISE study used 10 m surface reflectance, since the 5 m VENμS surface reflectance data product was unavailable then [20].

The PlanetScope constellation, operated by Planet Labs, comprises 180+ CubeSats in low Earth orbit, providing high-spatial-resolution observations on a near-daily revisit for monitoring land surface phenology. However, the utilization of PlanetScope data is often constrained by challenges related to sensor interoperability, cross-calibration, and atmospheric correction. The Planet Fusion product employs a comprehensive fusion methodology to address these challenges by inter-calibrating, harmonizing, and fusing multi-sensor PlanetScope data to generate a consistent sensor-agnostic daily surface reflectance dataset [26] that is interoperable with public mission multispectral satellites (Sentinel-2, Landsat 8/9). Planet Fusion processing includes temporally driven functionality related to cloud and cloud shadow masking, and gap-filling resulting in usable observations for every day.

The PlanetScope constellation consists of three generations of "Doves": Dove-Classic (2016–2022), Dove-R (2019–2022), and SuperDove (2020–). Dove-Classic is characterized by broad and partially overlapping spectral bands in the visible and near-infrared ranges. The Dove-R and SuperDove constellations have been improved to align with the visible and narrow NIR bands of Sentinel-2 [26]. Since the original PlanetScope data have been processed to the daily Planet Fusion data product, in this study, we utilized the Planet Fusion data product from 2019 and onwards to ensure that the analysis was conducted using a more consistent data stream. Table 2 includes the frequency of usable Planet observations before generating daily observations. This is the first study on the application of WISE to Planet Fusion.

Landsat, with 30-m-resolution optical bands, has long been essential for land cover mapping; however, its observations typically lack the temporal density required for precise land surface phenology mapping [27]. As indicated in Table 1, the average interval between usable Landsat-8 observations for this Maryland site in 2019 and 2020 surpassed 40 days. Following the launch of Landsat-9 in late 2021, there was an increase in revisit frequency and usable observations, with the frequency of usable observations boosted to less than 20 days. This enhancement offers possibilities for mapping crop emergence using Landsat data. In this assessment, we used Landsat data (L30) from HLS to investigate the detection of emergence.

ESA Sentinel-2 is an Earth observation mission designed to systematically acquire optical imagery over land and coastal waters [28]. The Sentinel-2 constellation, consisting of the Sentinel-2A and Sentinel-2B satellites, has provided 5-day revisit imagery over the study area since 2018. In our analysis, we utilized Sentinel-2 10 m data from 2019 to generate a map of green-up dates for analyzing the impact of spatial resolution. Sen2Cor was used to correct atmospheric effects and generate surface reflectance data [29]. To assess the impact of temporal frequency on emergence detection, we used the Sentinel-2 30-m-resolution data (S30) from HLS from 2019 to 2023. The results were compared to the 30-m-resolution results from the HLS and HLS L30 datasets.

The HLS dataset integrates Landsat and Sentinel-2 data through consistent atmospheric correction, cloud and cloud-shadow masking, geographic co-registration, common gridding, bidirectional reflectance distribution function normalization, and band-pass adjustment [30]. In our analysis, we utilized both the S30 and L30 30 m products from the HLS dataset to evaluate the impact of revisit frequency. One advantage of using HLS S30 over the original 10 m Sentinel-2 data is that it allows us to focus specifically on assessing the effect of temporal frequency. This approach reduces distractions arising from differences in data processing compared to Landsat, such as cloud masking, bidirectional reflectance

distribution function (BRDF) effects, and band-pass differences. This study utilized the HLS version 2.0 data products.

2.3. WISE Algorithm

The WISE algorithm is used here to assess the impact of spatial and temporal resolutions. The algorithm follows a two-step process for detecting crop emergence, as outlined in the original algorithm paper by Gao et al. [20]. The algorithm first generates a daily vegetation index (VI) time series and then employs the trend-based Moving Average Convergence and Divergence (MACD) method to identify crop emergence.

The daily VI is generated using the modified Savitzky–Golay (SG) filter technique. Instead of using the fixed length of the moving window in the traditional SG filter, our flexible implementation uses a fixed number of samples within a varying size of the moving window to keep local details yet still fill significant gaps.

The MACD method is utilized to identify increasing trends in the VI time series. This is achieved by computing the difference between two exponential moving averages, each characterized by a distinct length. Alongside the rising trend identified by MACD, the WISE algorithm also mandates an increasing trend in the mean VI time series. The algorithm records the transition (green-up) date and the rising momentum associated with each detected green-up. The momentum is a measure of the strength of a green-up event. For comprehensive details regarding the WISE methodology, readers are referred to the original algorithm paper by Gao et al. [20].

Since Planet Fusion has undergone gap filling, the daily VI can be directly computed from the original surface reflectance. In our evaluation, we compared the original daily VI time series with the smoothed VI time series. The smoothing process utilized the same Savitzky–Golay (SG) filter. We found similar green-up results with both methods. Subsequently, we turned off the smoothing process in applying the WISE algorithm to Planet Fusion data during later processing.

For VENμS, Sentinel-2, Landsat, and HLS data, we employed identical gap-filling parameters to those outlined in the original WISE paper [20], except for alfalfa. This involved requiring a minimum of 5 samples and a maximum searching window of 60 days in the flexible implementation of the SG filter. The gap-filling parameters were assessed in the previous study over the BARC area and found suitable for early VENμS, Sentinel-2, and HLS data [20].

Additionally, we utilized a minimum threshold of 0.01 as the green-up momentum to define a "meaningful" green-up event, consistent with the criteria specified in the original paper. The threshold of 0.01 for green-up momentum is a conservative value that can capture most green-up events for crops and natural vegetation. We selected the green-up event with maximum momentum from early April to late July to eliminate small variations caused by changes in soil conditions or noise. The maximum momentums for corn and soybeans were well above the minimum threshold (0.01) in our previous work. We adopted the same parameters and threshold in this study for a consistent comparison.

At the emergence stage, the Normalized Difference Vegetation Index (NDVI) and Enhanced Vegetation Index 2 (EVI2) tend to be low, and the saturation problem is not a concern. Previous research demonstrated that NDVI and EVI2 derived from VENμS data consistently captured similar green-up dates in 2019 [20]. In preparation for the current study, we investigated NDVI and EVI2 derived from Planet Fusion and HLS datasets using field observations collected in 2019, 2022, and 2023. Our analysis revealed that the mean biases and mean absolute differences (MADs) for NDVI and EVI2 were very close. In this paper, we utilize the NDVI time series to assess green-up detection across the six datasets.

For field-scale evaluations of crop emergence detection, surface reflectances were initially averaged for each field. NDVI was subsequently computed using the averaged surface reflectance from the red and near-infrared (NIR) bands. The WISE code was then executed field by field. Additionally, emergence detection was performed at the pixel scale using an NDVI time series derived from NDVI images at the original pixel resolution. At

this scale, we can generate a map of crop emergence dates, including sub-field variability in emergence.

2.4. Assessment Methods

Green-up dates were derived from VENμS, Planet Fusion, Landsat, Sentinel-2, and HLS time series using the WISE algorithm. The assessment was performed at both the field and pixel levels, utilizing ground emergence observations and planting records. We first analyzed a complex alfalfa field before extending the examination to all observed fields to evaluate the impact of varying temporal resolutions. Different aggregation methods at the field level were assessed to understand the impact of spatial resolution.

An alfalfa field in 2019 was used to evaluate the impact of temporal resolution. This field spanned 10.7 hectares (equivalent to over 120 HLS 30 m pixels) and was relatively uniform. Throughout the growing season, the alfalfa field was harvested four times and regrew after each harvest, presenting multiple growth cycles. This unique characteristic makes it an excellent case for testing remote sensing algorithms and time series analysis. Given alfalfa's relatively short regrowing periods, we modified the gap-filling parameters to require a minimum of 3 observations within 30 days in the flexible implementation of the SG filter. This modification aimed to capture the rapid changes in NDVI associated with alfalfa growth.

In the next step of analysis, we used 47 ground emergence observations collected in 2019, 2022, and 2023 to validate the field-scale green-up dates detected from the five datasets (methods used for aggregation to field scale are discussed below). Statistical metrics employed for validation included the mean difference (bias), mean absolute difference (MAD), root mean square error (RMSE), and coefficient of determination (R^2). We compared the results obtained from individual years and the combined data from all years.

The green-up dates detected from the five datasets were also compared to 115 planting records from 2019 to 2023. To identify possible outliers, including likely "too-early" and "too-late" detections, we utilized the accumulated growing degree days (AGDD) from the planting date to the green-up date.

Growing degree days (GDD) were computed using the difference between the mean and base temperatures. The mean temperature is the average of the daily minimum and maximum temperatures obtained from DayMet [24]. The base temperature represents the minimum development threshold for the crop. For corn and soybean, we set the effective temperature range to between 10 and 30 degrees Celsius for both the minimum and maximum temperatures and the base temperature to 10 degrees Celsius. The accumulated GDD (AGDD) for each field-year was calculated by summing the GDDs from the recorded planting date to the detected green-up date. Typically, corn and soybeans require at least 32 AGDD Celsius (or 90 degrees Fahrenheit) for emergence [31]. Possible "too-early" detections were defined as AGDD less than 32 °C Conversely, possible "too-late" detections were defined as AGDD greater than 150 °Cand with no green-up detected two weeks after planting. We then analyzed the percentage of detected green-ups and the percentage of outliers in the detection to assess the accuracy.

The impact of the spatial aggregation method at the field level was evaluated using Planet Fusion (3 m) and HLS (30 m) data. To achieve a field-level summary, we tested three aggregation approaches. The first approach was the default approach, which first averages the surface reflectance for each field and then computes NDVI for the field. The default approach was used to generate the results in Sections 3.1–3.3. The second approach first computes NDVI for each pixel and then averages NDVI across the field. The third approach generates a map of emergence dates for each pixel and then finds the median value of the green-up dates within the field. To assess the accuracy of these aggregation methods, we compared the results with ground emergence observations collected in 2019, 2022, and 2023. The maps of green-up dates generated from the five datasets were visually examined at their original image resolutions.

In contrast to the original WISE paper of Gao et al. [20], which compared green-up dates to the mid-date of the VE stage in 2019, this paper compares green-up dates to the first day of crop emergence. Additionally, while the original WISE paper utilized 10 m VENμS surface reflectances, this study employs 5 m VENμS surface reflectances. Furthermore, this study uses HLS version 2.0 data from 2019 to 2023, whereas the original WISE paper utilized version 1.4 in 2019 [20]. Consequently, the results obtained with the same sensor differ slightly from those in the original WISE paper.

3. Results

3.1. Performance over a Complex Case—Alfalfa

We utilize an alfalfa case to demonstrate the performance of different remote sensing time series. This case study presents complexity, since alfalfa was harvested four times between 7 May and 9 September 2019. After each harvest, the alfalfa plants regenerated and recovered their green appearance. Figure 2 illustrates how the four datasets (VENμS, Planet Fusion, Sentinel-2, and HLS) captured multiple green-up events throughout the growing season. Despite exhibiting different trends and magnitudes in the NDVI time series, the green-up dates detected by the four datasets are consistently close. However, Sentinel-2 missed a green-up date in mid-May due to a lack of cloud-free observations (no usable data in 65 days from 7 April to 14 June). HLS barely captured the mid-May green-up event, with the green-up momentum on May 15 being smaller than that in VENμS and Planet Fusion. This can be attributed to the absence of usable (cloud-free) HLS observations from 7 April to 23 May 2019. Landsat-8 faced challenges, with only four usable observations available between 1 April and 1 October 2019. As a result, Landsat-8 failed to generate a daily NDVI time series that was robust enough to detect any green-up events throughout the growing season.

3.2. Validation Using Ground Observations of Crop Emergence

The green-up dates of corn and soybeans were compared to the emergence dates observed on the ground in 2019, 2022, and 2023. Figure 3 shows the relationship between the ground-observed emergence days and detected green-up days from the five datasets. Generally, there is close agreement between the green-up and emergence dates, points clustering near the 1:1 line. Planet Fusion exhibits a strong correlation between the detected green-up dates and ground-observed emergence dates among the five datasets. However, it is essential to highlight that VENμS data are only available for 2019, limiting the scope of comparison. Additionally, the Landsat data failed to detect any green-up events for 2019, so Figure 3c only includes detections from 2022 and 2023.

Table 3 summarizes the statistical results from 47 field-years. VENμS (in 2019), Planet Fusion (all years), and HLS (all years) captured all green-ups. Sentinel-2 detected most green-ups, with a detection rate ranging from 81% to 91% across the three years. Planet Fusion performed slightly better than VENμS in 2019. The mean differences (bias) and mean absolute differences (MAD) from Planet Fusion were consistently less than three days and six days, respectively. The overall detection rate for Sentinel-2 from 47 field-year observations is 91%. Among the detected green-up events, the accuracies from Sentinel-2 and HLS are comparable to that of Planet Fusion, with biases of less than three days and an MAD of less than eight days each year. The HLS data detected all green-up events in three years, performing best in 2022 and worst in 2023. The coefficients of determination (R^2) for 2023 are lower, partially due to the smaller range of detected crop emergence dates. Overall, the R^2 values for all detected green-ups from 47 field-year observations are above 0.80 for Planet Fusion, Sentinel-2, and HLS.

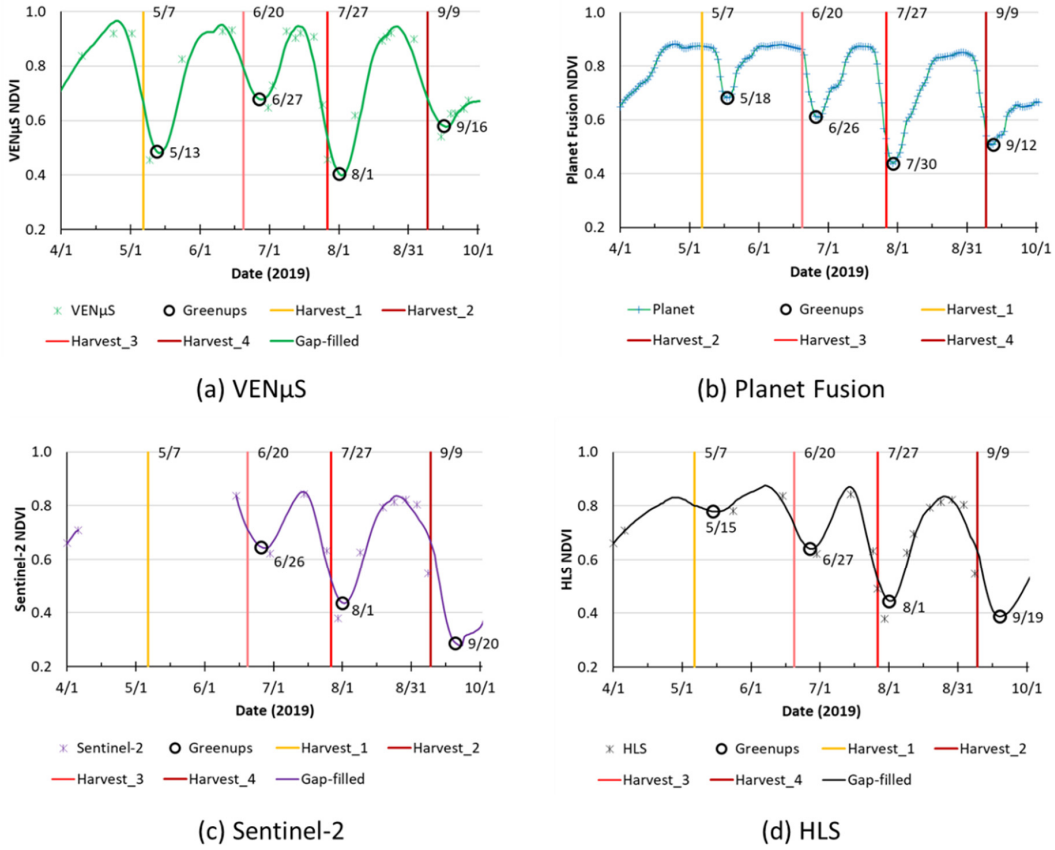

Figure 2. Green-up events detected using VENµS (**a**), Planet Fusion (**b**), Sentinel-2 (**c**), and HLS (**d**) for an alfalfa field in 2019. Sentinel-2 failed to detect green-up in the mid-May event. Landsat-8 failed to detect any green-up events and is omitted.

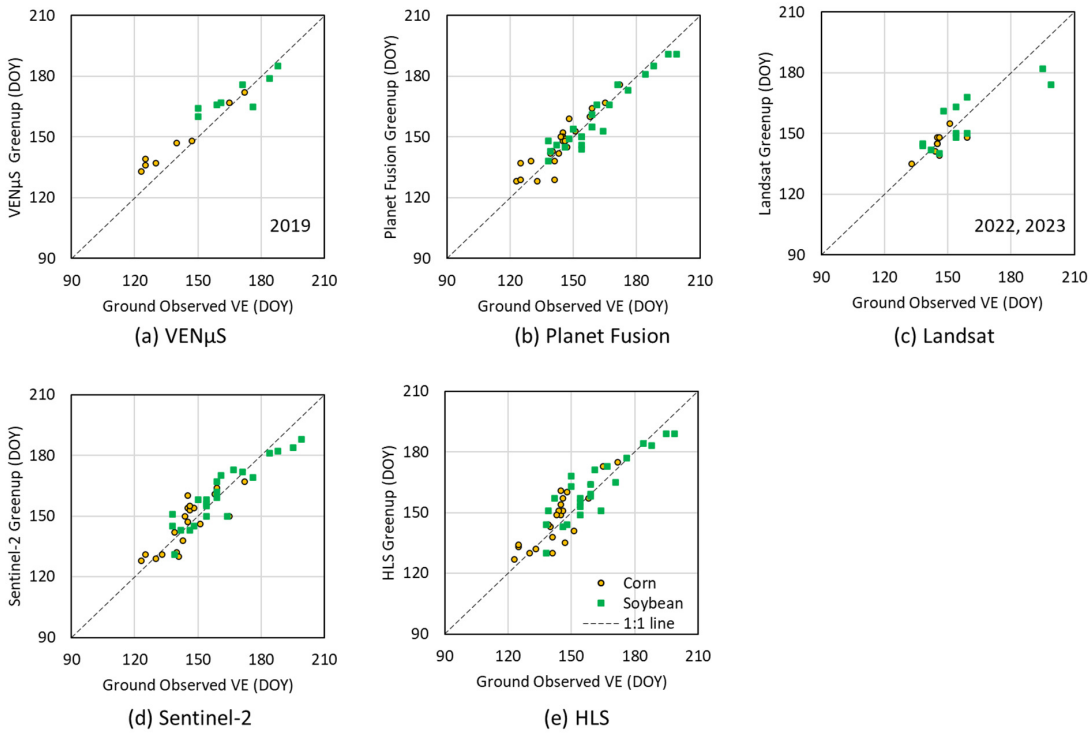

Figure 3. Scatter plots of the observed emergence days and green-up days detected using VENµS (**a**), Planet Fusion (**b**), Landsat (**c**), Sentinel-2 (**d**), and HLS (**e**).

Table 3. Summary of statistics for green-up dates detected from VENμS, Planet Fusion, Landsat, Sentinel-2 (S2), and HLS in comparison to the ground-observed emergence dates in 2019, 2022, 2023, and all years combined. (Diff: difference; MAD: mean absolute difference; RMSE: root mean squared error; R^2: coefficient of determination).

Year	Data Source	Percent Detected	Bias (Days)	Low Diff (Days)	High Diff (Days)	MAD (Days)	RMSE (Days)	R^2
2019	VENμS	100	4.7	−11.0	14.0	7.1	8.2	0.93
	PF	100	2.9	−3.0	12.0	4.3	5.0	0.97
	S2	81	−0.6	−15.0	9.0	6.3	7.2	0.88
	HLS	100	−0.9	−13.0	9.0	5.7	6.5	0.90
2022	PF	100	−1.2	−12.0	11.0	5.8	6.6	0.85
	Landsat	79	−2.0	−25.0	9.0	7.1	9.4	0.80
	S2	100	1.7	−11.0	15.0	6.1	7.5	0.82
	HLS	100	0.8	−11.0	16.0	5.6	7.1	0.87
2023	PF	100	0.8	−11.0	6.0	3.2	4.2	0.80
	Landsat	50	0.2	−7.0	13.0	5.5	6.8	0.48
	S2	100	−0.8	−14.0	9.0	5.5	6.5	0.64
	HLS	100	2.6	−13.0	15.0	7.8	8.8	0.28
All Years	PF	100	0.7	−12.0	12.0	4.6	5.5	0.88
	Landsat	44	−1.4	−25.0	13.0	6.6	8.7	0.73
	S2	91	0.4	−15.0	15.0	6.1	7.2	0.82
	HLS	100	2.2	−13.0	18.0	6.5	7.9	0.80

3.3. Assessment Using Crop Planting Records

We compared 115 crop planting records from 2019 to 2023 to the green-up dates detected from the five datasets. Figure 4 shows the scatter plots between the planting dates, observed emergence dates, and detected green-up dates. Note that VENμS only has results from 2019, and Landsat only includes results from 2021 to 2023. In the scatter plots, most green-up dates were observed to be later than the planting dates, appearing above the 1:1 line. The Planet Fusion, Sentinel-2, and HLS plots show a general trend that later plantings took less time to show green-ups. A similar trend is also observed in the planting emergence plot (Figure 4a), with a slope (0.9316) of linear fitting of less than one, presumably due to an accelerated seedling development rate at a later time (higher GDD levels). However, some exceptions are set apart from the 1:1 line trend. For example, there are seven field-years from Planet Fusion and 15 field-years from HLS that were detected earlier than the record planting dates. We further investigate the too-early and too-late cases in the following paragraphs.

In Figure 4c, the green-up date from Planet Fusion for field #1–9 in 2021 was detected 40 days after planting. The field was planted with corn on 29 April 2021, while the green-up date was detected on 8 June 2021. Further investigation into the NDVI dynamics, planting date, and the detected green-up date over this field (Figure 5a) shows that NDVI values at the planting and green-up dates were above 0.5. There was a long, flat period in NDVI after corn was planted. This is likely due to significant green weeds in the field and slow corn germination progress. Similarly, a late green-up date (33 days after planting) was also produced from HLS.

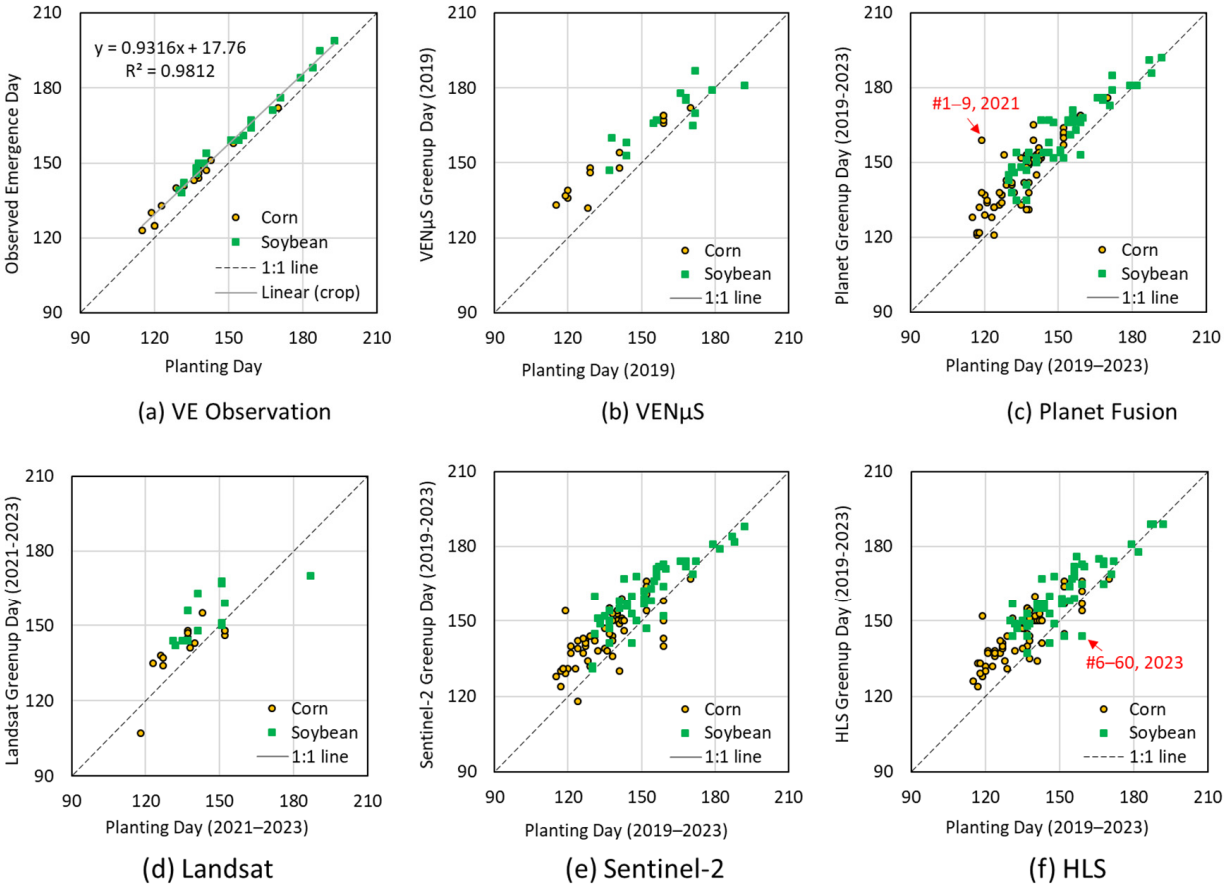

Figure 4. Scatter plots between the recorded planting dates and the observed emergence dates (**a**) and the detected green-up dates from 2019 to 2023 using VENμS (**b**), Planet Fusion (**c**), Landsat (**d**), Sentinel-2 (**e**), and HLS (**f**).

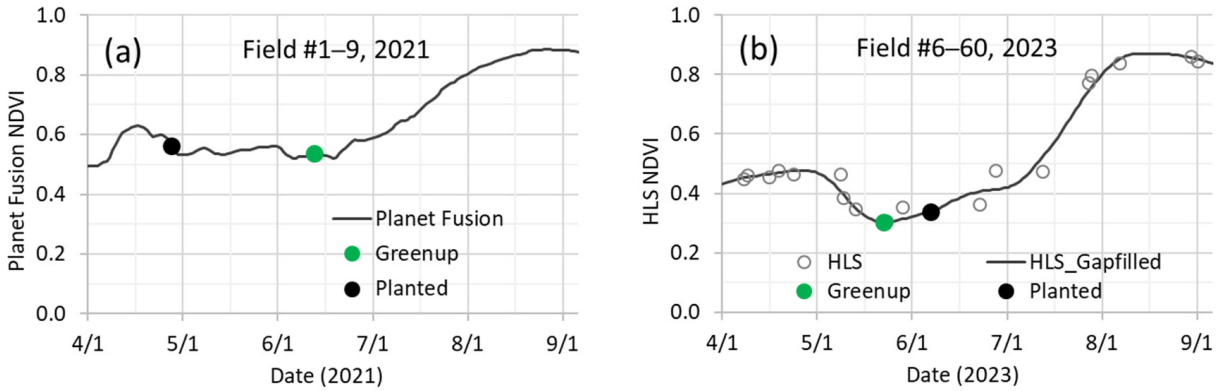

Figure 5. Outlier examples that detected green-up dates too late (**a**) (labeled in Figure 4b from Planet Fusion) or too early (**b**) (labeled in Figure 4e from HLS). Both cases have a flat low NDVI period.

In Figure 4f, the green-up date from HLS for field #6–60 in 2023 was detected 15 days before planting. This field was planted with soybeans on 8 June 2023. However, green-up was detected on 24 May 2023. Close examination of the HLS observations, the smoothed and gap-filled NDVI time series, the planting date, and the green-up date for field #6–60 (Figure 5b) reveals a long period with slowly increasing NDVI from mid-May to mid-June. The gap-filled NDVI time series increased in mid-May, leading to the early green-up detection. A too-early detection (6 days before planting) is also noticed for this case from

the Planet Fusion data. Both cases highlight the challenges of green-up detection during longer periods with minimal NDVI changes.

Exceptions in Figure 4 were further identified using the accumulated growing degree days (AGDD) from planting to green-up dates. Table 4 summarizes the results, highlighting possible too-early detections (AGDD < 32 C after planting date) and too-late detections (AGDD > 150 C and more than 2 weeks with no green-up after planting). Planet Fusion performed best among the five datasets, showing the highest detection rate and the lowest percentage of possible outliers (12% too-early and 15% too-late cases). Sentinel-2 and HLS show similar possible outliers (17–18% too-early and too-late cases). Landsat had the lowest detection rate, failing to detect any green-up events in 2019 and 2020 due to the limited availability of Landsat-8 data. With the launch of Landsat-9 in late 2021, the detection rate improved to 45%. Sentinel-2 produced results similar to HLS, with a slightly lower detection rate. The frequencies of usable observations for Sentinel-2 and HLS were approximately 8–10 days and 6–8 days, respectively, suggesting that, with the 10 days of usable observations, 95% of crop emergences could be detected.

Table 4. Summary of green-ups detected from five datasets with available observations and planting records.

Remote Sensing Dataset (Years Used)	Detection Rate (Percent of Detections)	Too-Early Cases (AGDD < 32 After Planting)	Too-Late Cases (AGDD > 150 and No Green-Up in 2 Weeks)	Coefficient of Determination (R^2)
VENμS (2019)	100%	14%	17%	0.89
Planet Fusion (2019–2023)	100%	12%	15%	0.85
Landsat (2021–2023)	45%	25%	14%	0.58
Sentinel-2 (2019–2023)	95%	18%	17%	0.75
HLS (2019–2023)	97%	18%	18%	0.79

3.4. Spatial Variability

The impact of the spatial resolution and aggregation methods was assessed using the Planet Fusion and HLS data. Table 5 summarizes the results of three different spatial aggregation methods: field-level averaging of surface reflectance (default approach), field-level averaging of NDVI, and calculating the field-level median of pixel-level green-up dates. Despite potential differences in the NDVI time series, no significant discrepancies were observed among the three approaches from the Planet Fusion and HLS datasets. Since NDVI is a non-linear form of reflectance, in theory, it cannot be averaged for mixed pixels. However, the fields observed in this study ranged from 2.5 to 16.5 hectares in size, making them relatively large and homogenous and making the spatial resolution less critical for field-level aggregation.

Although the results from the three aggregation approaches are close, the spatial variability at the sub-field scale is different. Figure 6 illustrates the map of crop emergence dates in 2019 obtained from Planet Fusion, VENμS, Sentinel-2, and HLS, all at their original spatial resolutions. The detected green-up dates for crops are consistent across the four datasets. However, experimental fields with mixed crop planting benefit from higher-spatial-resolution data. For instance, at the 3 m resolution of Planet Fusion, corn and soybean emergence dates in mixed planted fields are distinct in the zoomed-in maps in Figure 6a,e. The 5 m VENμS and 10 m Sentinel-2 datasets captured partial sub-field variabilities. In contrast, the 30 m HLS data could not detect sub-field details due to its lower spatial resolution.

Table 5. Statistics between emergence dates and green-up dates aggregated at field level from two datasets (Planet Fusion and HLS) and with three aggregation methods (averaged reflectance, averaged NDVI, and median green-up date) (where Diff: difference; MAD: mean absolute difference; RMSE: root mean squared error; R^2: coefficient of determination).

Dataset	**Planet Fusion**			**HLS**		
Aggregation Method	**Averaged Reflectance**	**Averaged NDVI**	**Median Green-Up**	**Averaged Reflectance**	**Averaged NDVI**	**Median Green-Up**
Bias	0.7	0.5	1.0	2.2	0.5	−0.1
Low Diff	−12.0	−12.0	−11.0	−13.0	−20.0	−23.0
High Diff	12.0	12.0	15.0	18.0	16.0	11.0
MAD	4.6	4.4	4.6	6.5	6.3	5.6
RMSE	5.5	5.3	5.6	7.9	7.6	7.0
R^2	0.90	0.90	0.89	0.80	0.80	0.83

Further investigation of the mixed fields (A and B in Figure 6e) revealed that the coarse-resolution time series of NDVI and surface reflectance at the field level could not detect any significant green-up during the growing season. This is because the mixed crops or planting dates smoothed the growing signals for the fields, and the WISE algorithm could not detect the upward trend for them. In order to assess the different aggregation methods, we removed the requirement for substantial green-up by revising the threshold of green-up momentum to zero (default 0.01). Table 6 lists the results for fields A and B from Planet Fusion and HLS. It shows that the green-up dates for field A differ for the different aggregation methods. Although field B generated similar green-up dates with the different aggregation methods, the 3 m green-up maps show two or three multimodal centers. This highlights the advantage of producing crop emergence at the original high spatial resolutions. The 30 m HLS could not detect the multimodal distribution. The performance of the WISE algorithm is somewhat related to the spatial resolution of the data sources for the mixed fields.

Table 6. Green-up dates aggregated at field level from two datasets (Planet Fusion and HLS) and with three aggregation methods (averaged reflectance, averaged NDVI, and median green-up date) for two mixed fields (A and B in Figure 6e).

Dataset	**Planet Fusion**				**HLS**		
Method	**Averaged Reflectance**	**Averaged NDVI**	**Median Green-Up**	**Multimodal Center**	**Averaged Reflectance**	**Averaged NDVI**	**Median Green-Up**
Field A	166	161	142	141,165	undetected	undetected	129
Field B	160	160	162	150,161,190	164	164	166

Green-up dates for forests produced from Sentinel-2 data were around mid-April, whereas other datasets indicated earlier green-up occurring from late March to early April. In 2019, the emergence of small tree leaves was observed on March 19 (day 78), followed by the appearance of large tree leaves on April 1 (day 91). Forest green-up dates from VENμS, Planet Fusion, and HLS appeared more consistent with the observed dates. The slightly later forest green-up dates from Sentinel-2 are likely due to the limited availability of usable Sentinel-2 observations during the early spring period.

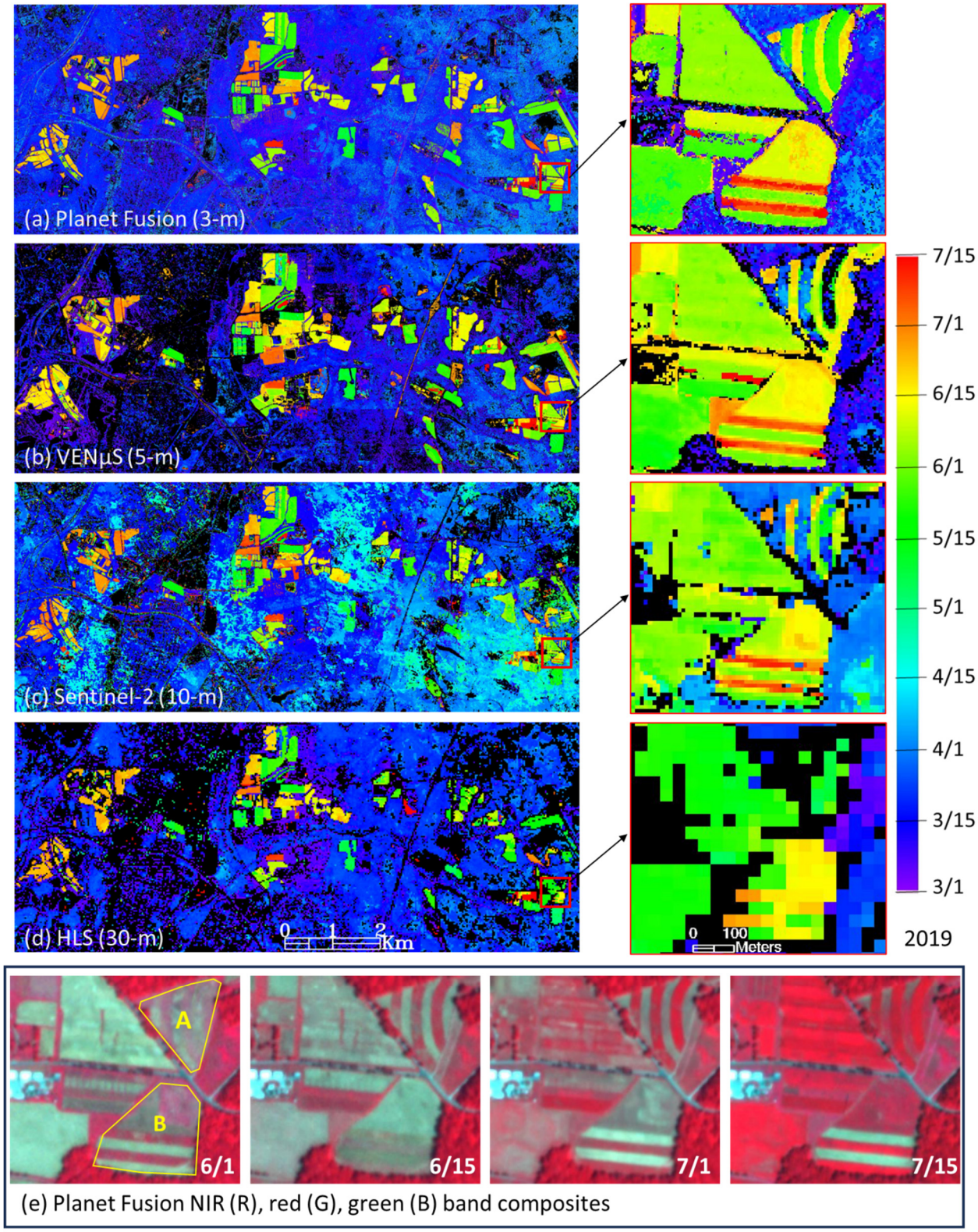

Figure 6. Green-up dates in 2019 from Planet Fusion (**a**), VENμS (**b**), Sentinel-2 (**c**), and HLS (**d**). The right panel shows the zoomed-in area with heterogeneous fields. The 3 m Planet Fusion captured the green-up of mixed crops. The 5 m VENμS and 10 m Senintel-2 detected some spatial variability, while the 30 m HLS lost most sub-field details. The Planet Fusion composite images (**e**) show the spatial and temporal heterogeneity (e.g., fields A and B) for the zoomed-in area.

4. Discussion

4.1. Impact of Revisit

This study assessed the requirement for satellite revisit cycles on crop emergence detection using five remote sensing datasets with varying revisits from daily to 16 days. Compared to the satellite revisit cycle, the frequency of usable observations, especially during the green-up period, is a more useful metric. Even though satellite revisit cycles for the same latitude are similar, the frequency of usable observations could differ due to cloud and snow coverage variations. In this study, we found that when the frequency of usable observations reached ten days, most crop emergence was detected, as shown in Figure 7.

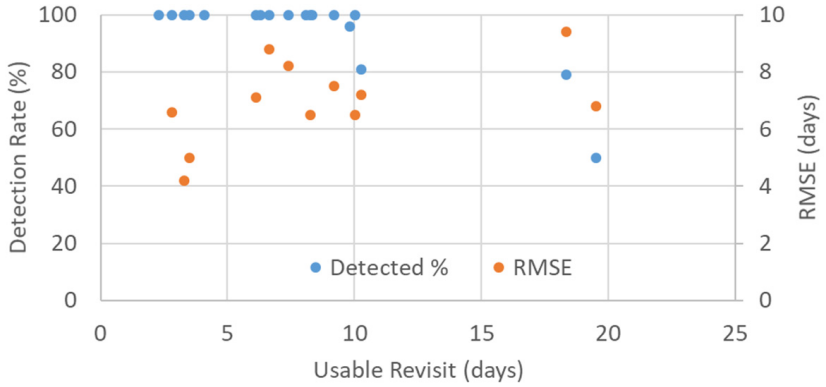

Figure 7. Relationship among detection rate (primary y-axis) and RMSE (secondary y-axis) of crop emergence and usable revisit for five datasets (VENμS, Planet Fusion, HLS L30, HLS S30, and HLS) from 2019 to 2023 (RMSE is calculated based on field observations from 2019, 2022, and 2023).

More frequent observations, particularly around the crop emergence stage, can improve emergence detection accuracy (smaller RMSE in Figure 7). Although the results were produced for a small area in Beltsville, Maryland, they represent the mid-Atlantic area in the US, with similar weather conditions.

Planet Fusion offers the most frequent observations (daily) and yields the highest detection rate, providing the most accurate results compared to ground-observed emergence dates and recorded planting dates. However, for large-area mapping, 3 m Planet data could be expensive. From a large-area operational standpoint, the 30-m-resolution HLS data would be more appropriate, as demonstrated in Corn Belt states by Gao et al. [21]. HLS data are freely available with a short latency period of 3–4 days. Moreover, HLS (30 m) processing requires only 1% of the computing power and disk storage needed to process Planet Fusion data (3 m). Despite this lower resolution, HLS still detects most green-ups and delivers satisfactory results.

4.2. Impact of Aggregation

The field-level crop emergence dates aggregated from different approaches appear similar in our study area. In theory, averaging surface reflectance first and then computing NDVI is the correct way to generate field-level NDVI time series. Since NDVI is a non-linear form of surface reflectance, it cannot be averaged to create a field-level NDVI. The aggregated NDVI values will differ from the two approaches if the field is heterogeneous. This study found no apparent difference in the crop emergence dates between the two aggregation approaches. This may be due to two reasons. One is that the observed fields included in our validation were relatively large and homogeneous. The second reason is that, even though NDVI was averaged, the NDVI time series was still temporally consistent and could be processed by WISE. However, aggregation methods should be used with caution for complex mixed fields. None of the single-value aggregation methods can describe the multimodal distribution of green-up dates.

Maps of green-up dates at the original resolution reveal variability in emergence dates within the field and could detect anomalies of emergence in the field. Since the median emergence date of a field from the emergence map is similar to the metrics used in the other two aggregation methods (surface reflectance and NDVI), we can first generate a map of crop emergence dates and run field-level aggregation later. The advantage is that the emergence mapping process can be performed in a stand-alone manner, especially when field polygons are not available in advance. In addition, the high-spatial-resolution map can preserve the multimodal distribution, even for crop-mixed fields.

4.3. Regional and Seasonal Impacts

In our experimental agricultural area, the temperature rose before the planting of summer crops, making temperature less influential. However, temperature could be a critical factor in crop emergence in agricultural production regions. Emergence can only occur after the AGDD reaches a minimum threshold. Including AGDD as a constraint factor can limit some too-early detections due to noise or variations in surface conditions in the early growing season. Such an approach could benefit areas (e.g., corn belt states) where crops are planted early and the temperature controls crop emergence.

Winter cash crops and cover crops, typically planted in the fall, exhibit less significant greening up than summer crops. Some may show greening up in the following spring, necessitating time series analysis across two years. The correlation between planting dates and emergence dates for winter cover crops can be weaker than for summer crops. Figure 8 demonstrates the NDVI time series and green-up dates for winter wheat and winter cover crops. Winter wheat was planted on 10 October 2020, and the green-up date was detected three weeks later, on 31 October 2020. The winter cover crop was planted on 18 October 2020. However, the green-up date was detected four months later, on 18 February 2021, due to the slow development of the winter cover crop.

4.4. Selection of Phenology Algorithms

Landsat surface phenology algorithms have been developed over several decades, with most approaches focusing on after-season analysis [22]. For example, threshold-based and curvature-based methods require multi-year time series data to map the phenology for a given target year [14,17,18]. They can provide information on multiple phenological stages (e.g., green-up and senescence). These methods are typically more suitable for research purposes. The derived land surface phenology is not directly related to the crop growth stages. By contrast, the shape-based approach can map crop growth stages in near-real time and even support short-term predictions [32], making it potentially valuable for monitoring multiple crop growth stages [33]. However, it requires knowledge of the time series patterns from previous years for each crop type and the current-year crop-type map. Early-season crop mapping can pose challenges and requires extra effort [34].

The WISE algorithm is a trend-based approach and requires only partial-year data. It is designed for operational application and can detect crop emergence within the growing season. This approach relies on clear observations during the early growth stages. It may not be able to detect crop emergence due to the lack of critical observations in near-real time. As a trend-based approach, the detection accuracy somewhat depends on the significance of green-up events. It is less effective for green-up events with a slowly increasing NDVI trend. In addition, WISE is not designed to map entire crop growth stages like shape-based approaches. WISE does not need to know the crop type in advance and can detect multiple green-up events during the growing season for specialty crops. While we have not compared different phenology approaches in this paper, the previous comparison found that threshold- and curvature-based methods identified green-up dates when two to four leaves appeared (V2–V4 stages) or 1–3 weeks after the crop emerged [19,22,32], while WISE can detect green-up dates a few days after emergence (VE stage) [20,21]. The green-up dates detected by WISE are closer to the VE stage.

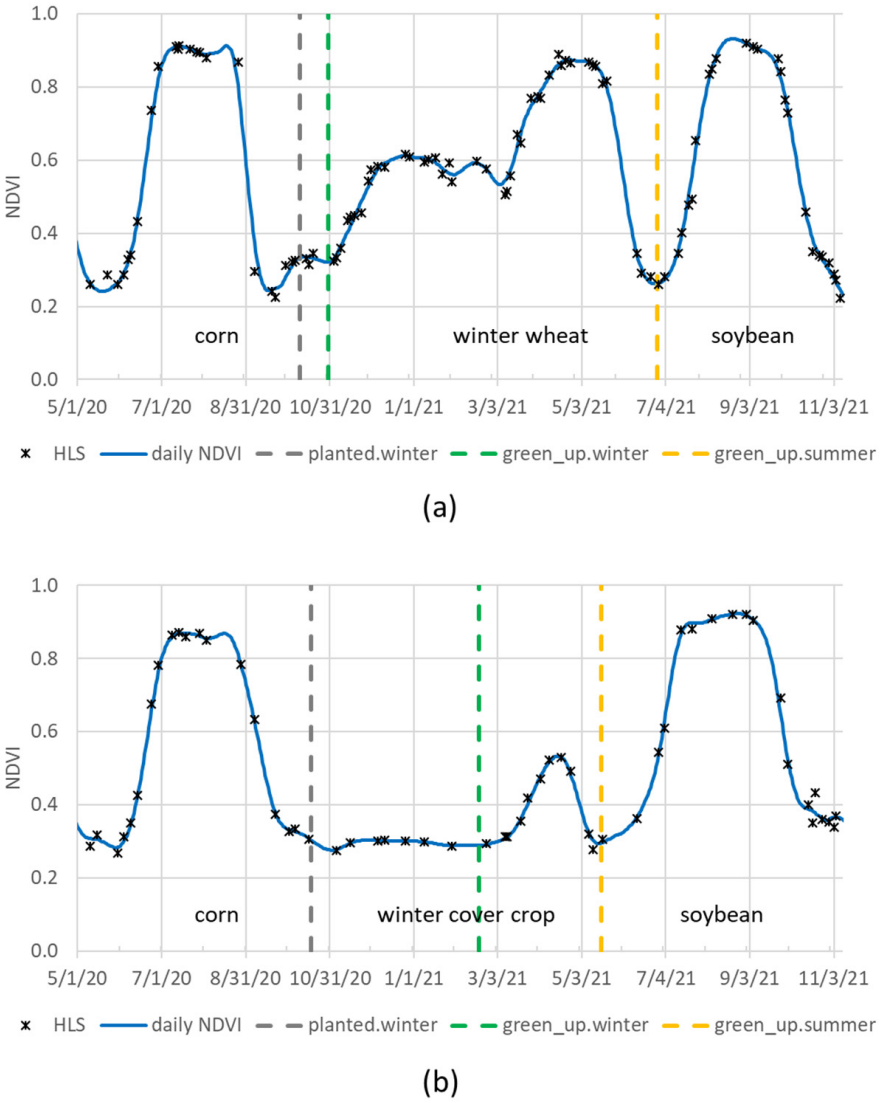

Figure 8. Green-up dates for winter wheat (**a**) and winter cover crop (**b**) detected from HLS. The winter cover crop was planted in the fall of 2020 but not established until the next spring, and the green-up date was detected on 18 February 2021.

4.5. Limitations

We demonstrate the impacts of the remote sensing temporal and spatial resolutions in crop emergence mapping using the WISE algorithm. The findings in this paper are based on our experimental research area in Beltsville, Maryland, USA. Regions with different weather conditions and field sizes may have different results. HLS provides high temporal resolutions for our area (US mid-Atlantic region). Regions with frequent cloud coverage may require more frequent observations. The performance of the WISE algorithm could be affected by the heterogeneity of the fields. WISE generated similar results for large homogeneous fields. However, the results vary for fields with mixed crops. Areas with mixed crops or small fields may require higher-spatial-resolution data.

This study evaluated the NDVI time series produced from several optical sensors. While optical sensors have recently been able to provide data with high spatial and temporal resolutions, their observations are still affected by clouds. Radar data, such as those from Sentinel-1, can provide all-weather observations and may be used to monitor crop emergence, especially in cloudy regions.

The WISE algorithm is a trend-based approach. The WISE algorithm works better when the field has green cover crops or weeds in early spring and is then terminated before summer crops are planted. However, detecting green-up from a slowly increasing trend in a time series in near-real time is still challenging.

5. Conclusions

Our experiment demonstrates that high temporal resolution is crucial in capturing crop emergence. The WISE algorithm successfully detected all green-ups using VENμS, Planet Fusion, and HLS data. Sentinel-2 detected 91% of green-ups overall, while Landsat detected approximately 45% of green-ups in 2022 and 2023, when both Landsat-8 and Landsat-9 were available. We found that 95% of emergences could be detected when the frequency of usable observations (i.e., cloud-free and snow-free) reached ten days per observation. The accuracies of detected emergence dates across the five datasets and three years were comparable, with overall mean differences (bias) of less than three days, mean absolute differences (MAD) of less than seven days, and root mean square errors (RMSE) of less than nine days. Planet Fusion (daily, 3 m) outperformed the rest of the datasets. It is particularly suitable for small or heterogeneous fields where sub-field variability is critical. While the 30 m spatial resolution of HLS (2–4 days) is suitable for large fields, it may lack sub-field details for smaller or heterogeneous fields. However, HLS data, being freely available, hold potential for operational applications for a large area. Further investigations need to be conducted in agricultural regions with different weather conditions and different crop types.

Author Contributions: Conceptualization, F.G.; methodology, F.G.; software, F.G.; validation, F.G.; formal analysis, all authors; investigation, all authors; resources, all authors; data curation, all authors; writing—original draft preparation, F.G.; writing—review and editing, all authors; visualization, F.G. All authors have read and agreed to the published version of the manuscript.

Funding: This research received no external funding.

Data Availability Statement: The data presented in this study are available on request from the corresponding author.

Acknowledgments: This research was a contribution from the Long-Term Agroecosystem Research (LTAR) network. LTAR is supported by the United States Department of Agriculture. The USDA is an equal opportunity provider and employer. Any use of trade, firm, or product names is for descriptive purposes only and does not imply endorsement by the US Government. The findings and views described herein do not necessarily reflect those of Planet Labs PBC.

Conflicts of Interest: The authors declare no conflicts of interest. The funders had no role in the design of the study; in the collection, analyses, or interpretation of the data; in the writing of the manuscript; or in the decision to publish the results.

References

1. Kucharik, C.J. A multidecadal trend of earlier corn planting in the central USA. *Agron. J.* **2006**, *98*, 1544–1550. [CrossRef]
2. Walthall, C.L.; Hatfield, J.; Backlund, P.; Lengnick, L.; Marshall, E.; Walsh, M.; Adkins, S.; Aillery, M.; Ainsworth, E.A.; Ammann, C.; et al. *Climate Change and Agriculture in the United States: Effects and Adaptation*; USDA Technical Bulletin 1935; USDA: Washington, DC, USA, 2012; 186p. Available online: https://www.usda.gov/sites/default/files/documents/CC%20and%20Agriculture%20Report%20(02-04-2013)b.pdf (accessed on 10 September 2024).
3. Moulin, S.; Bondeau, A.; Delecolle, R. Combining agricultural crop models and satellite observations: From field to regional scales. *Int. J. Remote Sens.* **2010**, *19*, 1021–1036. [CrossRef]
4. Deines, J.M.; Swatantran, A.; Ye, D.; Myers, B.; Archontoulis, S.; Lobell, D.B. Field-scale dynamics of planting dates in the US Corn Belt from 2000 to 2020. *Remote Sens. Environ.* **2023**, *291*, 113551. [CrossRef]
5. Zhou, Q.; Guan, K.; Wang, S.; Hipple, J.; Chen, Z. From satellite-based phenological metrics to crop planting dates: Deriving field-level planting dates for corn and soybean in the U.S. Midwest. *J. Photogramm. Remote Sens.* **2024**, *216*, 259–273. [CrossRef]
6. Yang, Y.; Anderson, M.C.; Gao, F.; Johnson, D.M.; Yang, Y.; Sun, L.; Dulaney, W.; Hain, C.; Otkin, J.A.; Prueger, J.; et al. Phenological corrections to a field-scale, ET-based crop stress indicator: An application to yield forecasting across the U.S. Corn Belt. *Remote Sens. Environ.* **2021**, *257*, 112337. [CrossRef]

7. Lobell, D.B.; Ortiz-Monasterio, J.I.; Sibley, A.M.; Sohu, V.S. Satellite detection of earlier wheat sowing in India and implications for yield trends. *Agric. Syst.* **2013**, *115*, 137–143. [CrossRef]
8. NASS Field Crops Usual Planting and Harvesting Dates, USDA NASS Agricultural Handbook No.628. Available online: https://www.nass.usda.gov/Publications/Todays_Reports/reports/fcdate10.pdf (accessed on 10 September 2024).
9. NASS Crop Progress Report. Available online: http://www.nass.usda.gov/Publications/National_Crop_Progress/ (accessed on 10 September 2024).
10. Liu, Y.; Bachofen, C.; Wittwer, R.; Duarte, G.S.; Sun, Q.; Klaus, V.H.; Buchmann, N. Using PhenoCams to track crop phenology and explain the effects of different cropping systems on yield. *Agric. Syst.* **2022**, *195*, 103306. [CrossRef]
11. LTAR Phenocam. 2024. Available online: https://ltar.ars.usda.gov/data/data-access/data-phenocams/ (accessed on 10 September 2024).
12. Browning, D.M.; Russell, E.S.; Ponce-Campos, G.E.; Kaplan, N.; Richardson, A.D.; Seyednasrollah, B.; Spiegal, S.; Saliendra, N.; Alfieri, J.G.; Baker, J.; et al. Monitoring agroecosystem productivity and phenology at a national scale: A metric assessment framework. *Ecol. Indic.* **2021**, *131*, 108147. [CrossRef]
13. Friedl, M.; Henebry, G.M.; Reed, B.; Huete, A.; White, M.; Morisette, J.; Nemani, R.; Zhang, X.Y.; Myneni, R. Land Surface Phenology. A Community White Paper requested by NASA. 2006. Available online: https://cce.nasa.gov/mtg2008_ab_presentations/Phenology_Friedl_whitepaper.pdf (accessed on 10 September 2024).
14. Gray, J.M.; Sulla-menashe, D.; Friedl, M.A. User Guide to Collection 6 MODIS Land Cover Dynamics (MCD12Q2) Product. Available online: https://modis-land.gsfc.nasa.gov/pdf/MCD12Q2_Collection6_UserGuide.pdf (accessed on 10 September 2024).
15. Zhang, X.Y.; Friedl, M.A.; Schaaf, C.B.; Strahler, A.H.; Hodges, J.C.F.; Gao, F.; Reed, B.C.; Huete, A. Monitoring vegetation phenology using MODIS. *Remote Sens. Environ.* **2003**, *84*, 471–475. [CrossRef]
16. Zhang, X.Y.; Jayavelu, S.; Liu, L.L.; Friedl, A.M.; Henebry, G.M.; Liu, Y.; Schaaf, C.; Richardson, A.D.; Gray, J. Evaluation of Land Surface Phenology from VIIRS Data using Time Series of PhenoCam Imagery. *Agric. For. Meteorol.* **2018**, *256–257*, 137–149. [CrossRef]
17. Zhang, X.Y.; Friedl, M.A.; Henebry, G.M. *VIIRS/NPP Land Cover Dynamics Yearly L3 Global 500 m SIN Grid V001*; NASA EOSDIS Land Process; DAAC: Greenbelt, MD, USA, 2020. [CrossRef]
18. Bolton, D.K.; Gray, J.M.; Melaas, E.K.; Moon, M.; Eklundh, L.; Friedl, M.A. Continental-scale land surface phenology from harmonized Landsat 8 and Sentinel-2 imagery. *Remote Sens. Environ.* **2020**, *240*, 111685. [CrossRef]
19. Gao, F.; Anderson, M.C.; Zhang, X.Y.; Yang, Z.W.; Alfieri, J.G.; Kustas, W.P.; Mueller, R.; Johnson, D.M.; Prueger, J.H. Toward mapping crop progress at field scales through fusion of Landsat and MODIS imagery. *Remote Sens. Environ.* **2017**, *188*, 9–25. [CrossRef]
20. Gao, F.; Anderson, M.; Daughtry, C.; Karnieli, A.; Hively, D.; Kustas, W. A within-season approach for detecting early growth stages in corn and soybean using high temporal and spatial resolution imagery. *Remote Sens. Environ.* **2020**, *242*, 111752. [CrossRef]
21. Gao, F.; Anderson, M.C.; Johnson, D.M.; Seffrin, R.; Wardlow, B.; Suyker, A.; Diao, C.; Browning, D.M. Towards Routine Mapping of Crop Emergence within the Season Using the Harmonized Landsat and Sentinel-2 Dataset. *Remote Sens.* **2021**, *13*, 5074. [CrossRef]
22. Gao, F.; Zhang, X. Mapping Crop Phenology in Near Real-Time Using Satellite Remote Sensing: Challenges and Opportunities. *J. Remote Sens.* **2021**, *2021*, 8379391. [CrossRef]
23. Dulaney, W.P.; Anderson, M.C.; Gao, F.; Stern, A.; Moglen, G.; Meyers, G.; Daughtry, C.S.T.; White, W.; Akumaga, U.; Showalter, J. Development of a gridded yield data archive for farm management and research at the USDA Beltsville Agricultural Research Center. *Agrosystems Geosci. Environ.* **2024**, *7*, e20474. [CrossRef]
24. Daymet. *Daily Surface Weather Data on a 1-km Grid for North America, Version 4 R1*; DRNL DAAC: Oak Ridge, TN, USA, 2024. [CrossRef]
25. Dedieu, G.; Hagolle, O.; Karnieli, A.; Ferrier, P.; Crébassol, P.; Gamet, P.; Desjardins, C.; Yakov, M.; Cohen, M.; Hayun, E. VENμS: Performances and first results after 11 months in orbit. In Proceedings of the 2018 IEEE International Geoscience and Remote Sensing Symposium, Valencia, Spain, 22–27 July 2018. [CrossRef]
26. Planet Fusion Team. *Planet Fusion Monitoring Technical Specification*, Version 1.3.0; Planet Fusion Team: San Francisco, CA, USA, 2021; Available online: https://support.planet.com/hc/en-us/articles/4406292582673-Planet-Fusion-Monitoring-Technical-Specification.html (accessed on 10 September 2024).
27. Radeloff, V.C.; Roy, D.P.; Wulder, M.A.; Anderson, M.; Cook, B.; Crawford, C.J.; Friedl, M.; Gao, F.; Gorelick, N.; Hansen, M.; et al. Need and vision for global medium-resolution Landsat and Sentinel-2 data products. *Remote Sens. Environ.* **2024**, *300*, 113918. [CrossRef]
28. European Space Agency (ESA) Sentinel-2 Mission Guide. Available online: https://sentiwiki.copernicus.eu/web/s2-mission (accessed on 10 September 2024).
29. Sen2Cor. Available online: https://step.esa.int/main/snap-supported-plugins/sen2cor/ (accessed on 10 September 2024).
30. Claverie, M.; Ju, J.; Masek, J.G.; Dungan, J.L.; Vermote, E.F.; Roger, J.C.; Skakun, S.V.; Justice, C. The Harmonized Landsat and Sentinel-2 surface reflectance data set. *Remote Sens. Environ.* **2018**, *219*, 145–161. [CrossRef]
31. Cropwatch. University of Nebraska—Lincoln. Available online: https://cropwatch.unl.edu/growing-degree-units-and-corn-emergence (accessed on 10 September 2024).

32. Liu, L.; Zhang, X.; Yu, Y.; Gao, F.; Yang, Z. Real-time monitoring of crop phenology in the midwestern United States using VIIRS observations. *Remote Sens.* **2018**, *10*, 1540. [CrossRef]
33. Diao, C.; Yang, Z.; Gao, F.; Zhang, X.; Yang, Z. Hybrid phenology matching model for robust crop phenological retrieval. *ISPRS J. Photogramm. Remote Sens.* **2021**, *181*, 308–326. [CrossRef]
34. Li, H.; DI, L.; Zhang, C.; Lin, L.; Guo, L.; Yu, E.G.; Yang, Z. Automated in-season crop-type data layer mapping without ground truth for the Conterminous United States based on multisource satellite imagery. *IEEE Trans. Geosci. Remote Sens.* **2024**, *62*, 1–14. [CrossRef]

Disclaimer/Publisher's Note: The statements, opinions and data contained in all publications are solely those of the individual author(s) and contributor(s) and not of MDPI and/or the editor(s). MDPI and/or the editor(s) disclaim responsibility for any injury to people or property resulting from any ideas, methods, instructions or products referred to in the content.